JOURNAL OF PROPULSION AND POWER
Vol. 24, No. 3, May–June 2008

Outlet-Boundary-Condition Influence for Large Eddy Simulation of Combustion Instabilities in Gas Turbines

S. Roux*
Centre Européen de Recherche et de Formation Avancée en Calcul Scientifique, 31057 Toulouse, France
M. Cazalens†
Société Nationale d'Etude et de Construction de Moteurs d'Aviation, 77550 Reau, France
and
T. Poinsot‡
Institut de Mécanique des Fluides de Toulouse, 31400 Toulouse, France

DOI: 10.2514/1.33739

Large eddy simulations of combustion require more precise boundary conditions than classical Reynolds-averaged methods. This study shows how the reacting flow within a gas turbine combustion chamber can be influenced by the description of the downstream boundary. Large eddy simulation calculations are performed on a combustion chamber terminated by a high-pressure stator containing vanes in which the flow is usually choked and submitted to strong rotation effects. High-pressure stators are present in all real gas turbines, but they are often not computed and are simply replaced by a constant-pressure-outlet condition. This study compares a large eddy simulation calculation in which the high-pressure stator is replaced by a constant-pressure-outlet surface and a large eddy simulation in which the high-pressure stator is included in the computational domain and explicitly computed. The comparison of the flow in the chamber in both large eddy simulations reveals that the presence of the high-pressure stator modifies the mean flow in the second part of the chamber but does not affect the primary combustion zone. The unsteady field, on the other hand, is strongly affected by the high-pressure stator. Results demonstrate that the high-pressure stator should be included in realistic large eddy simulations of combustion chambers for gas turbines.

Introduction

LARGE eddy simulation (LES) is a promising technique to study combustion in complex-geometry burners [1–6]. Specifying boundary conditions for such flows has long been viewed as a second-order question. Many recent studies prove that boundary conditions are actually becoming a first-order issue, especially to predict combustion instabilities. Two different types of configurations must be considered: academic burners and real gas turbines. In academic burners in which combustion chambers are fed through a plenum and discharge into the atmosphere, boundary conditions can be unambiguously specified simply by including the plenum into the computation domain and a part of the outside atmosphere [7]. For such geometries with a compressible LES solver, not only the mean flow, but also the possible acoustic unstable modes, can be captured [8,9]. In real gas turbine configurations in which a compressor and a turbine are installed upstream and downstream of the combustion chamber, the problem is much more difficult, and where to begin and end the computational domain is by no means obvious.

In the present paper, the problem of inlet conditions will not be discussed and the computational domain will include only the plenum, not the geometry upstream of the plenum. The study will focus on the influence of downstream conditions; in gas turbines, the combustion chamber gases flow through a high-pressure stator (HPS) when entering the turbine. This high-pressure stator contains vanes in which the flow is usually choked and rather difficult to compute, especially with LES formulations. Therefore, many LES of gas turbine chambers stop before the HPS in a section in which the flow is still reasonably slow and the influence of the condition imposed in this section (usually an imposed pressure) is hoped to be negligible. In other words, the HPS is simply not considered and its influence is assumed to be small.

To evaluate the influence of the HPS on LES results, the present paper presents LES of the combustion chamber of an aircraft gas turbine using two different boundary conditions for the outlet. In the first computation, the HPS is not included and the computational domain stops upstream of its position. In the second case, the HPS is included. The comparison between the two cases allows evaluation of the exact effect of the HPS on the flow through the combustion chamber, both in terms of mean flow and acoustic activity.

LES of Reacting Flows

The LES code used to performed the two computations solves the full compressible Navier–Stokes equations on parallel computers.[§] It can handle hybrid (structured and unstructured) meshes and is thus well adapted to the complexity of industrial combustor geometries. The wall-adapting linear eddy (WALE) model [10] is used to describe the subgrid stresses. The turbulence/combustion interaction is modeled by the thickened-flame model [11–15]. The space discretization uses a finite volume formulation with cell-vertex formulation and the code is explicit in time. The numerical scheme used here has a second-order spatial accuracy.

Received 27 July 2007; revision received 30 January 2008; accepted for publication 31 January 2008.

*Research Engineer, Computational Fluid Dynamics Combustion Team, 42 Avenue G. Coriolis.
†Combustion Design Reviewer, 2 Road Point Rene Ravaud.
‡Professor, Allée du Professeur C. Soula. Member AIAA.

§Data available online at http://www.cerfacs.fr/cfd/ [retrieved 20 March 2008].

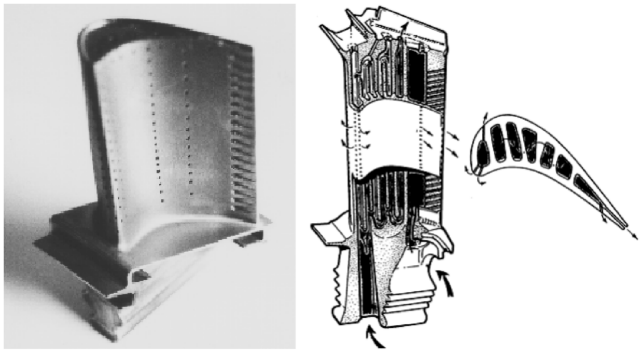

Fig. 1 Photograph of one blade of a HPS with small holes injecting fresh air to cool it (left) and the cooling scheme of a HPS (right).

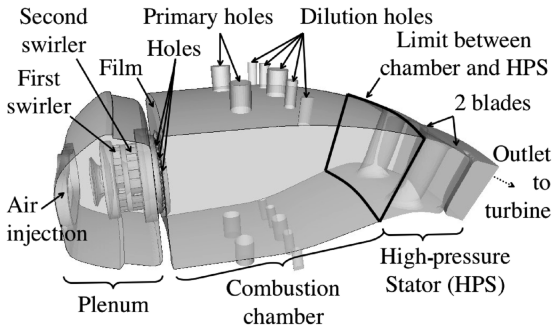

Fig. 2 Three-dimensional view of the plenum, the combustion chamber, and the HPS for a 20-deg sector; external and internal walls are multiperforated.

Configurations

Geometry

The HPS is the first row of blades met by the flow at the exit of the combustion chamber (Fig. 1). These blades do not move with the combustor axis: they are static. The thermal strain supported by the HPS imposes the use of cold air to cool its surface metal [16]. Even if the main role of the HPS is to deviate the flow, it can also considerably modify acoustic conditions at the exit of the combustion chamber.

The combustor chosen for this study is annular. It contains 18 burners installed in 18 identical sectors of 20 deg. To reduce computational costs, LES is performed on a single sector with periodic boundary conditions (Fig. 2). The first air circuit feeds a cavity called the plenum, which in turn feeds two corotating swirlers composed of 12 vanes, as well as 26 holes protecting the upstream wall of the combustion chamber from the flame. The fuel (JP10) is injected along the axis of the burner to be mixed with the air coming from the swirlers. Figure 2 shows the combustor, its injection system (also detailed in Fig. 3), and the HPS.

Two unstructured meshes have been generated to study the influence of the HPS. Both begin at the plenum inlet, but the first one ends at the exit of the combustion chamber and the second one ends after the HPS. The two meshes are refined on the most important zones of the computation: the injector in which the mixing takes place and the reaction zone (Fig. 4).

Table 1 Mass flow rates injected in a 20-deg angular sector of the simulated combustor

Injection	Mass flow rate, kg/s
Dilution	0.704
Injector: air	0.174
Injector: fuel (JP10)	0.026

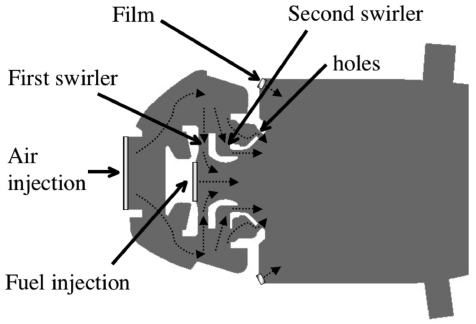

Fig. 3 Detail of the injection, axial cut.

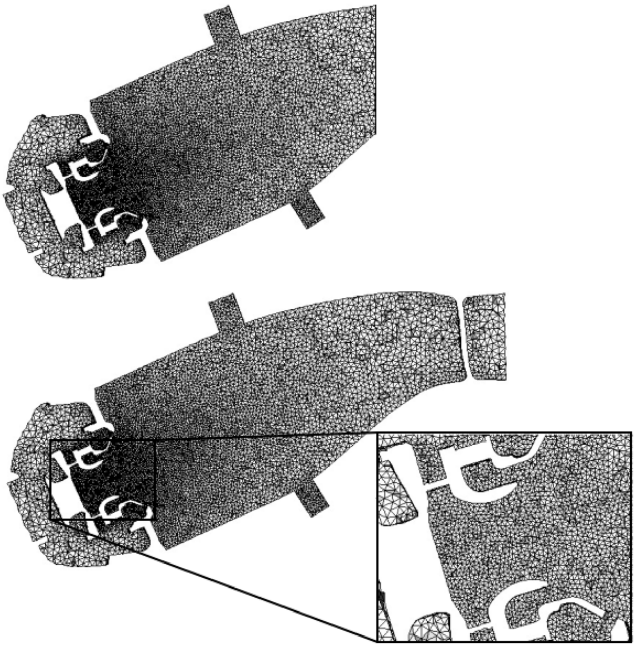

Fig. 4 View of the meshes for the two cases: without HPS (top) and with HPS (bottom).

Boundary Conditions

The injected air and the fuel are at a temperature of 473 K. Inlet-boundary mass flow rates are given in Table 1. These Navier–Stokes characteristic boundary conditions are nonreflective [17]. At the outlet, a pressure condition imposes 4.4 bars in the combustion chamber in the two cases. At the bottom of the injector, velocity and equivalence-ratio profiles are imposed to simulate the presence of the fuel atomizer (Fig. 5).

A specific wall law [18,19] is used to impose the porosity, the injection angle, and the mass flow rate injected through the multiperforated walls. It has an effect on results but has not been studied here in detail. On the walls, adiabatic wall laws are imposed [9].

Meshes and CPU Costs

The two meshes contain about 400,000 nodes and 2,000,000 cells, leading to a time step of around 0.17 ms. In terms of CPU cost, the reduced efficiency of the LES (computation time in microseconds/iteration/node) is about 2.1 and computations are run on 32 processors. An IBM BladeCenter cluster of 2.2 Tflops was used.[¶]

Combustion

The chemical model used for this simulation consists of a one-step kinetic scheme with an adjusted preexponential constant in the

[¶]Data available online at http://www.cerfacs.fr/Info/resources/IBM/IBM.jpg [retrieved 20 March 2008].

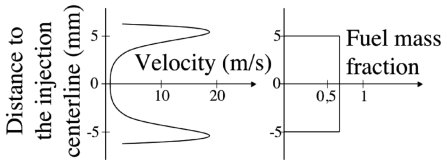

Fig. 5 Velocity profiles (left) and mass fraction profiles (right) of the fuel injection.

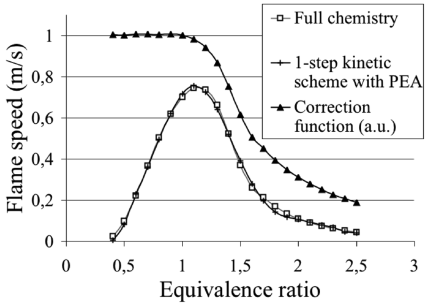

Fig. 6 One-dimensional flame: evolution of the flame speed for the JP10 at 4.4 bars.

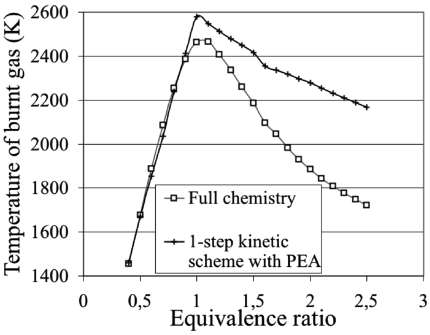

Fig. 7 One-dimensional flame: evolution of the burned gas temperature for the JP10 at 4.4 bars.

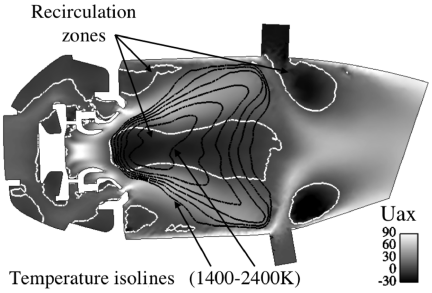

Fig. 8 Field of mean axial velocity: zero axial mean velocity isoline (white lines) and temperature isolines (black lines).

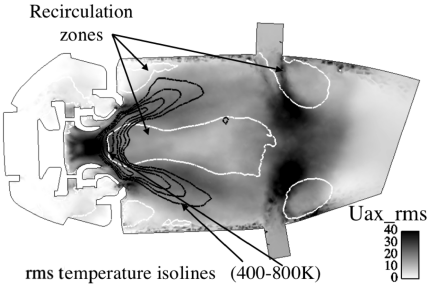

Fig. 9 Field of axial velocity fluctuations: zero axial mean velocity isoline (white lines) and temperature-fluctuation isolines (black lines).

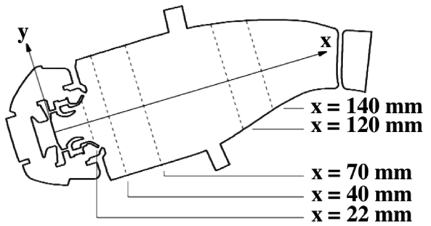

Fig. 10 Positions of the five profiles in which fields are compared for the computations with/without the HPS.

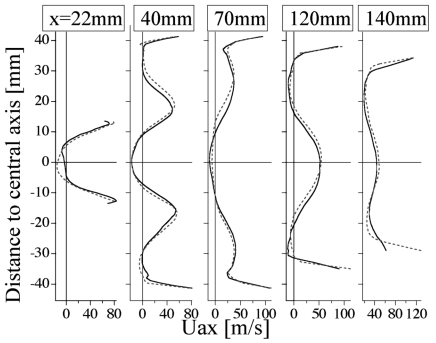

Fig. 11 Mean axial velocity profiles without HPS (solid line) and with HPS (dashed line).

Arrhenius law. This method, which can be seen as a simplification of Linan's technique [20], is called the preexponential adjusted (PEA) method and is used to impose the behavior of one-step chemical schemes in the rich zone. The reaction rate is as follows:

$$\dot{\omega} = A(\phi) Y_F^{nF} Y_O^{nO} e^{-Ta/T} = A_0 f(\phi) Y_F^{nF} Y_O^{nO} e^{-Ta/T} \qquad (1)$$

where $f(\phi)$ is the correction function to be defined later, $A_0 = 7.84 \times 10^{14}$ cgs, $nF = 1.5$, $nO = 0.55$, and Ta is the activation temperature associated with the activation energy $Ea = 3 \times 10^4$ cal/mol. The temperature of fresh gas is 473 K and the pressure is 4.4 bar.

One-dimensional flames have been used as a test case: from the differences between flames obtained with a complex kinetic scheme (36 species and 174 reactions) [21] and with the one-step PEA scheme, it is possible to fit the $f(\phi)$ function as the square root of the real flame speed divided by the flame speed resulting from the one-step kinetic scheme. Figures 6 and 7 show the laminar flame speed and maximum temperature obtained with the full scheme and the one-step PEA scheme. The agreement for the flame speed is excellent. The correction function $f(\phi)$ is 1 for all lean regimes and goes rapidly to zero on the rich side (Fig. 6). Discrepancies are observed for the adiabatic flame temperature on the rich side, but they remain acceptable for the present exercise.

Comparison of Results with and Without HPS

Mean Flow

The mean axial velocity field looks similar for both cases (with/without HPS). As a consequence, it is only shown for the case without HPS (Fig. 8). It is possible to distinguish several recirculation zones. The flame is concentrated between the bottom of the combustion chamber and the dilution holes, inducing high levels of temperature fluctuations (Fig. 9). Sections have been placed along the central axis of the chamber (Fig. 10) to compare mean and rms profiles of the main variables of the flow (Figs. 11–14, 5, and 16–18.

Two zones of the combustion chamber can be distinguished. The first one contains the injector and the first part of the combustion chamber ($x < 120$ mm). In this zone, only small differences exist between the two computations, and profiles obtained with or without HPS are close. In the downstream part of the combustion chamber

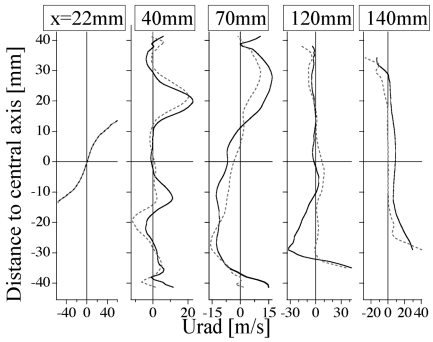

Fig. 12 Mean radial velocity profiles without HPS (solid line) and with HPS (dashed line).

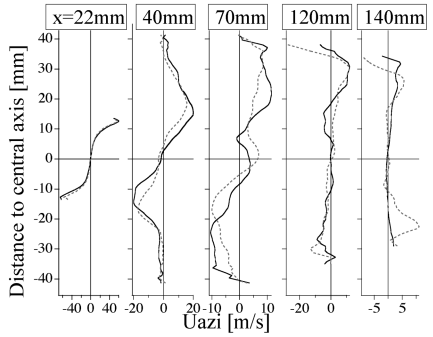

Fig. 13 Mean azimuthal velocity profiles without HPS (solid line) and with HPS (dashed line).

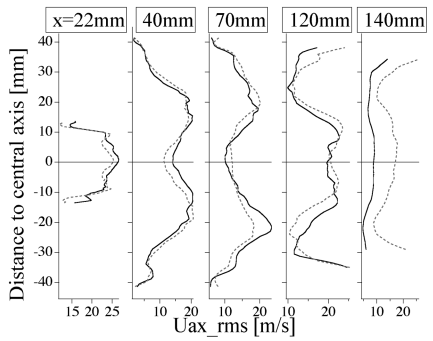

Fig. 14 The rms axial velocity profiles without HPS (solid line) and with HPS (dashed line).

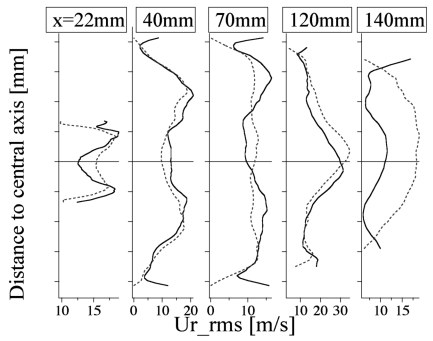

Fig. 15 The rms radial velocity profiles without HPS (solid line) and with HPS (dashed line).

($x > 140$ mm), differences appear between the calculations with and without HPS. The axial velocity, for instance, presents higher oscillations when the HPS is taken into account (Fig. 14). The same observation is true for radial (Fig. 15) and azimuthal (Fig. 16) rms velocity profiles, which are 5 to 10 times higher with the HPS.

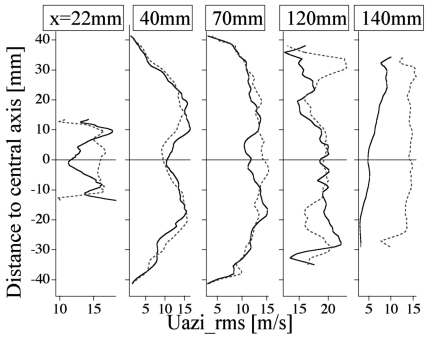

Fig. 16 The rms azimuthal velocity profiles without HPS (solid line) and with HPS (dashed line).

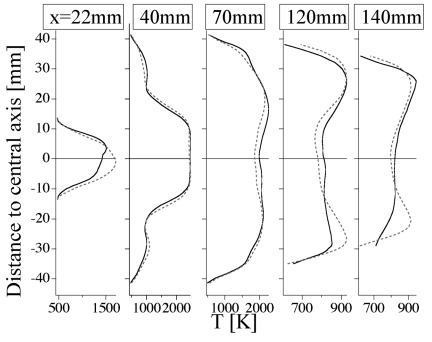

Fig. 17 Mean temperature profiles without HPS (solid line) and with HPS (dashed line).

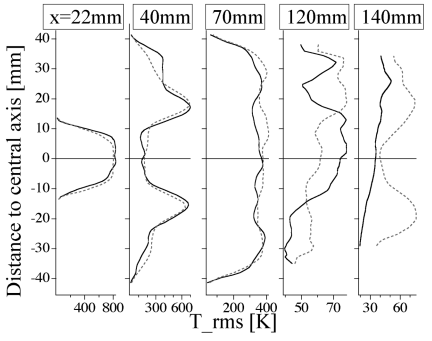

Fig. 18 rms temperature profiles without HPS (solid line) and with HPS (dashed line).

The mean temperature is also rather different at $x = 120$ and 140 mm (Fig. 17), showing that the outlet profile at the exit of the combustion chamber is affected by the presence of the HPS. It is important to notice this, because outlet temperature profiles are one of the main results used in practice to design combustion chambers. Likewise, temperature fluctuations are obviously underestimated when the HPS is not included into the computational domain (Figs. 18–22).

These comparisons show that the HPS plays an important role in the second part of the combustion chamber but has a limited influence on the primary zone. In an industrial context, it is therefore vital to take the HPS into account in the LES, because the characteristics of the flow at the exit of the combustion chamber are used to design the combustor.

Flame Structure

The flame structures obtained with both computations are similar (Fig. 23). The flame swirls around the fuel injection, which is rotating because of the two corotative swirlers of the injector. The flame is wrinkled and flaps and moves back and forth along the central axis of the combustion chamber.

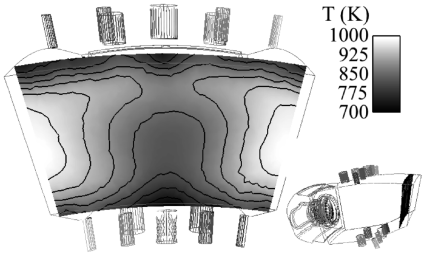

Fig. 19 Mean temperature field close to the exit of the combustion chamber; simulation without HPS.

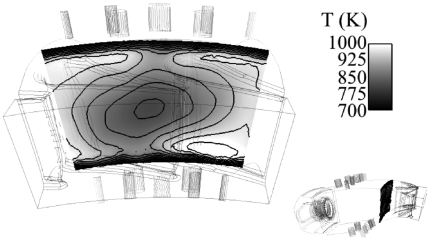

Fig. 20 Mean temperature field close to the exit of the combustion chamber; simulation with HPS.

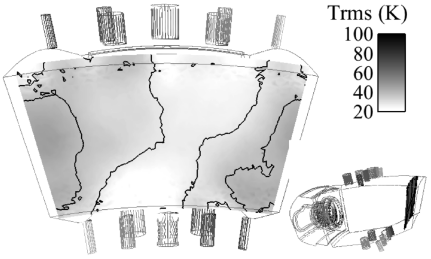

Fig. 21 The rms temperature field close to the exit of the combustion chamber; simulation without HPS.

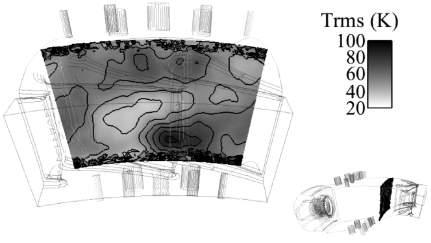

Fig. 22 The rms temperature field close to the exit of the combustion chamber; simulation with HPS.

To highlight the flame structure, Fig. 24 displays the value of the Takeno index

$$T_{ak} = \frac{\nabla Y_{JP10} \cdot \nabla Y_{O_2}}{|\nabla Y_{JP10} \cdot \nabla Y_{O_2}|}$$

on the flame in the central plane of the burner [22]. This index is equal to 1 in zones in which premixed fuel is burning, and it is equal to −1 in diffusion flame zones. The first flame elements are premixed and burn the rich mixture in the primary zone. When the hot unburned fuel mixed with combustion products then meets the fresh air injected through the primary and dilution holes and through the multiperforated walls, a diffusion flame forms (Fig. 24), as indicated by the negative values of the Takeno index and by the fact that the flame lies along the stoichiometric line.

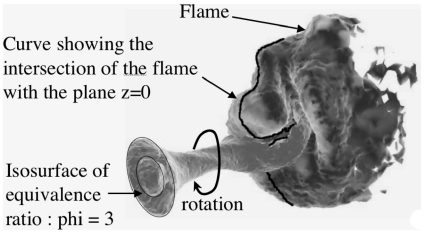

Fig. 23 Flame topology.

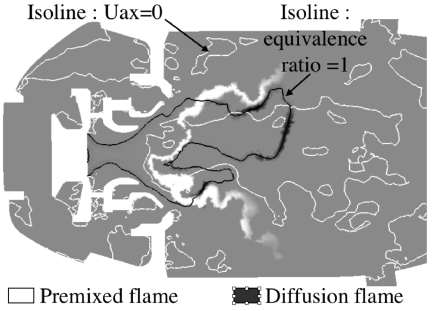

Fig. 24 Field of Takeno index in the burner central plane.

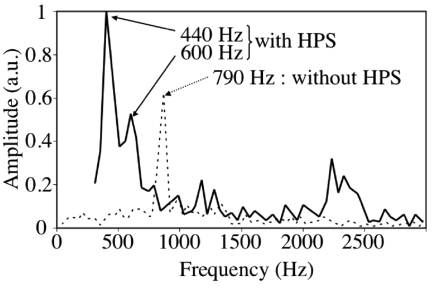

Fig. 25 Fourier spectrum of the pressure fluctuations in the combustion chamber; without HPS, amplitude of $P_{\text{rms}} = 3000$ Pa; with HPS, amplitude of $P_{\text{rms}} = 5500$ Pa.

Unsteady Activity

From the pressure signal in the combustion chamber, it is possible to identify the main oscillation modes of the combustion chamber (Fig. 25); results are fundamentally different between the cases with and without the HPS. The frequencies and the number of instability frequencies depend on the outlet-boundary conditions. Without the HPS, a single mode at 790 Hz is observed. With the HPS, two modes at 440 and 600 Hz appear.

Conclusions

This study is based on the comparison of the reacting flow within a combustion chamber of a gas turbine with and without an HPS (high-pressure stator). LES results show that the influence of the HPS on mean quantities (temperature, species, and velocity profiles) is strong in the second part of the chamber, but remains limited in the primary zone. On the other hand, when unsteady effects are considered, including the HPS leads to significant differences: a modal analysis of the amplitude and frequencies of the most intense modes reveals considerable differences when the HPS is included in the computation. Even though including the HPS in a high-fidelity LES is an expensive exercise, it can be concluded that it is vital to correctly predict unsteady combustion in gas turbines.

References

[1] Di Mare, F., Jones, W. P., and Menzies, K., "Large Eddy Simulation of a Model Gas Turbine Combustor," *Combustion and Flame*, Vol. 137,

No. 3, 2004, pp. 278–295.
doi:10.1016/j.combustflame.2004.01.008

[2] Pitsch, H., and Duchamp de la Geneste, L., "Large Eddy Simulation of Premixed Turbulent Combustion Using a Level-Set Approach," *Proceedings of the Combustion Institute*, Vol. 29, Elsevier, Amsterdam, 2002, pp. 2001–2005.

[3] Selle, L., Lartigue, G., Poinsot, T., Koch, R., Schildmacher, K.-U., Krebs, W., Prade, B., Kaufmann, P., and Veynante, D., "Compressible Large-Eddy Simulation of Turbulent Combustion In Complex Geometry on Unstructured Meshes," *Combustion and Flame*, Vol. 137, No. 4, 2004, pp. 489–505.
doi:10.1016/j.combustflame.2004.03.008

[4] Poinsot, T., and Veynante, D., *Theoretical and Numerical Combustion*, 2nd ed., R.T. Edwards, Philadelphia, 2005.

[5] Pitsch, H., "Large-Eddy Simulation of a Turbulent Combustion," *Annual Review of Fluid Mechanics*, Vol. 38, 2006, pp. 453–482.
doi:10.1146/annurev.fluid.38.050304.092133

[6] Freitag, M., and Janicka, J., "Investigation of a Strongly Swirled Premixed Flame Using LES," *Proceedings of the Combustion Institute*, Vol. 31, Elsevier, Amsterdam, 2007, pp. 1477–1485.

[7] Roux, S., Lartigue, G., Poinsot, T., Meier, U., and Bérat, C., "Studies of Mean and Unsteady Flow in a Swirled Combustor Using Experiments, Acoustic Analysis and Large Eddy Simulations," *Combustion and Flame*, Vol. 141, Nos. 1–2, 2005, pp. 40–54.
doi:10.1016/j.combustflame.2004.12.007

[8] Selle, L., Benoit, L., Poinsot, T., Nicoud, F., and Krebs, W., "Joint Use Of Compressible Large-Eddy Simulation and Helmoltz Solvers for the Analysis of Rotating Modes in an Industrial Swirled Burner," *Combustion and Flame*, Vol. 145, No. 1–2, 2006, pp. 194–205.
doi:10.1016/j.combustflame.2005.10.017

[9] Schmitt, P., Poinsot, T., Schuermans, B., and Geigle, K., "Large-Eddy Simulation and Experimental Study of Heat Transfer, Nitric Oxide Emissions and Combustion Instability in a Swirled Turbulent High Pressure Burner," *Journal of Fluid Mechanics*, Vol. 570, 2007, pp. 17–46.
doi:10.1017/S0022112006003156

[10] Nicoud, F., and Ducros, F., "Subgrid-Scale Stress Modelling Based on the Square of the Velocity Gradient," *Flow, Turbulence and Combustion*, Vol. 62, No. 3, 1999, pp. 183–200.
doi:10.1023/A:1009995426001

[11] Angelberger, C., Egolfopoulos, F., and Veynante, D., "Large Eddy Simulations of Chemical and Acoustic Effects on Combustion Instabilities," *Flow, Turbulence and Combustion*, Vol. 65, No. 2, 2000, pp. 205–220.
doi:10.1023/A:1011477030619

[12] Colin, O., Ducros, F., Veynante, D., and Poinsot, T., "A Thickened Flame Model for Large Eddy Simulations of Turbulent Premixed Combustion," *Physics of Fluids*, Vol. 12, No. 7, 2000, pp. 1843–1863.
doi:10.1063/1.870436

[13] Légier, J.-P., Poinsot, T., and Veynante, D., "Dynamically Thickened Flame Large Eddy Simulation Model For Premixed and Non-Premixed Turbulent Combustion," *Proceedings of the Summer Program*, Center for Turbulence Research, Stanford, CA, 2000, pp. 157–168.

[14] Angelberger, D., Veynante, D., Egolfopoulos, F., and Poinsot, T., "Large Eddy Simulations of Combustion Instabilities in Premixed Flames," *Proceedings of the Summer Program*, Center for Turbulence Research, Stanford, CA, 1998, pp. 61–82.

[15] Légier, J.-P., "Simulations Numériques des Instabilités de Combustion dans les Foyers Aéronautiques," Ph.D. Thesis, Inst. National Polytechnique, Toulouse, France, 2001.

[16] Mattingly, J., *Elements of Gas Turbine Propulsion*, McGraw–Hill, New York, 1996.

[17] Selle, L., Nicoud, F., and Poinsot, T., "The Actual Impedance of Non-Reflecting Boundary Conditions: Implications for the Computation of Resonators," *AIAA Journal*, Vol. 42, No. 5, 2004, pp. 958–964.
doi:10.2514/1.1883

[18] Mendez, S., Eldredge, J., Nicoud, F., Poinsot, T., Shoeybi, M., and Iaccarino, G., "Numerical Investigation and Preliminary Modeling of a Turbulent Flow over a Multi-Perforated Plate," *Proceedings of the Summer Program*, Center for Turbulence Research, Stanford, CA, 2006, pp. 57-72.

[19] Mendez, S., Nicoud, F., and Poinsot, T., "Large-Eddy Simulations of a Turbulent Flow Around a Multi-Perforated Plate," *Complex Effects in Large Eddy Simulations*, Lecture Notes in Computational Science and Engineering, Vol. 56, Springer, Berlin, 2006, pp. 289–303.

[20] Fernandez, E., Sanchez, A., Linan, A., and Williams, F., "A Simple One-Step Chemistry Model for Partially Premixed Hydrocarbon Combustion," *Combustion and Flame*, Vol. 147, Nos. 1–2, 2006, pp. 32–38.
doi:10.1016/j.combustflame.2006.08.001

[21] Li, S., Varatharajan, B., and Williams, F., "Chemistry of JP-10 Ignition," *AIAA Journal*, Vol. 39, No. 12, 2001, pp. 2351–2356.

[22] Yakhot, A., Orszag, S., Yakhot, V., and Israely, M., "Renormalization Group Formulation of Large-Eddy Simulation," *Journal of Scientific Computing*, Vol. 4, No. 2, 1989, pp. 139–158.
doi:10.1007/BF01061499

J. Oefelein
Associate Editor